ISSN 1028-334X, Doklady Earth Sciences, 2007, Vol. 417, No. 8, pp. 1281–1286. © Pleiades Publishing, Ltd., 2007.
Original Russian Text © A.V. Klyuchevskii, V.M. Dem'yanovich, 2007, published in Doklady Akademii Nauk, 2007, Vol. 417, No. 2, pp. 245–250.

GEOPHYSICS

Stressed State of the Medium in the Lithosphere of the Baikal Rift Zone Based on the Data of Seismic Moments of Large Earthquakes

A. V. Klyuchevskii and V. M. Dem'yanovich

Presented by Academician G.S. Golitsyn February 7, 2007

Received February 6, 2007

DOI: 10.1134/S1028334X07080351

Investigation of the spatial structure of the stressed state of the medium in the lithosphere of the Baikal Rift System (BRS) at the hierarchy level of large earthquakes ($11 \le K_P \le 14$) showed that a riftogenesis regime with shock-related dip-slip faulting (hereafter, normal faulting) exists in the region at the realization probability $P_N \ge 0.5$, while local regions of increased probability of strike-slip faulting and reverse faulting ($P \ge 0.25$) determine the zones of the nonuniform deformed state of the medium. The analysis of the dynamics of stresses in the lithosphere of the region confirms the dominating role of riftogenesis in seismotectonic processes. However, this dominant is not stable and approximate equality and even short-period domination of strike-slip faulting and reverse faulting were recorded at the end of the 1980s and beginning of the 1990s.

Seismic, seismological, and regional multidisciplinary studies showed that geostructural shapes and geodynamical processes (including modern motions in the lithosphere) are caused by endogenous transformations in deep spheres of the Earth [1]. Study of the peculiarities of the structure and properties of the lithosphere using geophysical methods allows us to distinguish the general properties of the spatial location of geological structures and regularities of the dynamic interaction between lithospheric plates and blocks, which result in earthquakes. Since the spatial location of the zones of seismic hazard is governed first of all by the stressed-strained state of the lithosphere, the rheology of the medium, and the tendency of the action of tectonophysical forces in the region, understanding of the deep geological structure and modern geodynamic situation is crucial for investigation of the regularities and evolution of seismic process in any seismoactive region. Understanding of the structure and dynamics of the stressed-strained state of the lithosphere at the level of hierarchy of large earthquakes is especially pressing in light of modern tendencies of forecasting large earthquakes and controlling seismic processes, which are based on knowledge of the properties and peculiarities of the system of regional seismogenesis. They start with the gathering of information about the state of the system, its relations, and logic of functioning.

At present, studies of the stressed-strained state of the medium in the lithosphere of the BRS based on seismological data commonly use focal parameters of large earthquakes with energy class $K_P \ge 10$ [1–4] and parameters of earthquakes sources with $K_P \ge 7$ [5–7]. The parameters of earthquake sources in the Baikal region are calculated for Brune's source model [8] based on the method presented in [9]. The application of seismic moments of tectonic earthquakes for the reconstruction of the stress field is based on the following fact: the moment is related to the motion along the fracture [10, 11], whose type, in turn, is specified by the relation between principal stresses in the lithosphere [12]. Using the data on 143 earthquakes ($11 \le K_P \le 14$), which occurred in the region from 1968 to 1994 and have the determination of the focal mechanism, we calibrated the average level over the class of the logarithm of seismic moment $\overline{M}_O$ by the type of motion in the source (Table 1). After this, the initial sampling of 802 earthquakes with $11 \le K_P \le 14$ was divided into shocks related to normal faulting ($n = 501$), strike-slip faulting ($n = 145$), and reverse faulting ($n = 156$) of different energy classes according to the $\log\overline{M}_O$ level. It is worth noting the high representativeness of the factual material. The seismic moments were determined almost for 100% of earthquakes ($n = 802$, $11 \le K_P \le 14$) recorded in the Baikal region ($\varphi = 48°$–$60°$ N, $\lambda = 96°$–$122°$ E) from 1968 to 1994. Formalization was made for the entire dataset based on the assumption that

Institute of the Earth's Crust, Siberian Division, Russian Academy of Sciences, ul. Lermontova 128, Irkutsk, 664033 Russia; e-mail: akluchev@crust.irk.ru

Calibrated values of the logarithm of mean seismic moment $\log \overline{M}_O$ of large earthquakes in the BRS with $K_P \geq 11$ corresponding to the transition from one type of motion in the source to the other type

Class	Normal faulting	Oblique faulting	Strike-slip faulting	Reverse strike-slip faulting	Number of calibrated shocks			
	$\log \overline{M}_O$				normal faulting	strike-slip faulting	reverse faulting	total
11	22.5	22.65	22.8	22.95	28	4	11	43
12	23.15	23.3	23.45	23.6	29	9	6	44
13	23.7	23.8	23.9	24.0	23	6	7	36
14	24.1	24.2	24.3	24.5	11	7	2	20

strong shocks of different energy classes reflect the correlated character of the behavior of the stress system in the study range of K_P: the ratio of the number of normal faulting, strike-slip faulting, and reverse faulting to the total number of earthquakes in the spatiotemporal sampling characterized the realization probability of shocks of such a type. It is worth noting that this condition is not fulfilled for weak shocks, while spatiotemporal mismatch between the formation of the types of motions is observed in the sources of microshocks ($K_P = 7$ and $K_P = 8$) and larger earthquakes ($K_P = 9$ and $K_P = 10$) [6]. In the total sampling of data, the realization probability of dip-slip faulting, strike-slip faulting, and reverse faulting is equal to $P_N \approx 0.63$, $P_S \approx 0.18$, and $P_R \approx 0.19$, respectively.

Figure 1 presents a chart of epicenters and contour lines of the density of epicenters of 802 earthquakes with $11 \leq K_P \leq 14$ in a grid of $1.0° \times 1.0°$ to give an idea about the spatiotemporal and energetic structure of the initial materials. One can see that the contour lines of the density of epicenters of shocks $N \geq 3$ cover the entire territory of the BRS. The inset in Fig. 1a shows a histogram of the distribution of the number of earthquakes in time and energy class. An increase in the number of earthquakes is observed in the histogram during the geodynamic activation at the end of the 1970s and the beginning of the 1980s and at the end of the 1980s and beginning of the 1990s. The mean number of earthquakes is approximately 30 events per year. The data in Fig. 1 indicate a good spatiotemporal representativeness of the used materials.

Figure 2 presents a chart of contour lines of the realization probability of normal faultings P_N, strike-slip faulting P_S, and reverse faulting P_R obtained at the number of shocks $n \geq 3$ in an averaging area of $1.5° \times 1.5°$. The chart shows that the region dominated by normal faulting $P_N \geq 0.5$ extends through the BRS from the southwest to the northeast along the rift structures and is separated in the central part of Lake Baikal (the Akademicheskaya Isthmus area between Ol'khon Island and Svyatoi Nos Peninsula). The distribution of P_N at the northeastern flank is quite simple with a linear dominant along the rift depressions. In the southwestern area, a region of high probability of normal faulting $P_N \geq 0.5$ extends to the south up to the Bolnai Fault and Selenga River in Mongolia. The zone of increased probability of strike-slip faulting $P_S \geq 0.35$ is localized in the Akademicheskaya Isthmus area, marked by the separation of contour lines of probability $P_N \geq 0.5$. A complex structure of increased probability of strike-slip faulting $P_S \geq 0.25$–0.35 is distinguished at the southwestern flank. The Baikal region incorporates several large zones, where the realization probability of reverse faulting is $P_R \geq 0.25$. At the southwestern flank, three zones with P_R surround the Khubsugul rift system. The Akademicheskaya Isthmus area includes a zone with $P_R \geq 0.25$, which coincides with the strike-slip fault zone with $P_S \geq 0.35$. A few small regions of increased realization of strike-slip faulting and reverse faulting spread over the territory characterize the hierarchic structure and spatial coordination of inhomogeneities in the stressed-strained state of the medium in the lithosphere of the BRS.

The inset (Fig. 2A) presents graphs of the annual mean realization probability P of shocks for all types of motions along the faults. Graphs before 1981 are constantly dominated by normal faulting at a mean level of $P_N \approx 0.7$–0.8 and approximately equal probabilities of normal faulting and reverse faulting: $P_S \approx P_R \approx 0.1$–$0.15$. In 1982, the realization probability of normal faulting decreased to $P_N \approx 0.48$, the probability of shock-related reverse faulting (hereafter, reverse faulting) increased to $P_R \approx 0.33$, and the probability of shock-related strike-slip faulting (hereafter, strike-slip faulting) was $P_S \approx 0.19$. In the next year, the probability of normal faulting began to increase and reached $P_N \approx 0.75$ in 1984, while $P_S \approx 0.17$ and $P_R \approx 0.08$. In 1987, the level of probability of normal faulting dropped to $P_N \approx 0.25$, while $P_S \approx 0.50$ and $P_R \approx 0.25$. The time interval between 1990 and 1994 is characterized by approximately the same realization probability of shocks of different types of motions along the fault. In 1994, the realization proba-

Fig. 1. Chart of epicenters and contour lines of density of epicenters for 802 earthquakes in the BRS with $11 \le K_P \le 14$. The inset (A) presents a histogram of the distribution of shocks in time and energy class. (*1*) Faults, (*2*) depressions, (*3*) lakes, (*4*) contour lines of density of shock epicenters; (*5*) energy class according to the T.G. Rautian scale and type of motion along the fracture (circles denote normal faulting; boxes, strike-slip faulting; and triangles, reverse faulting).

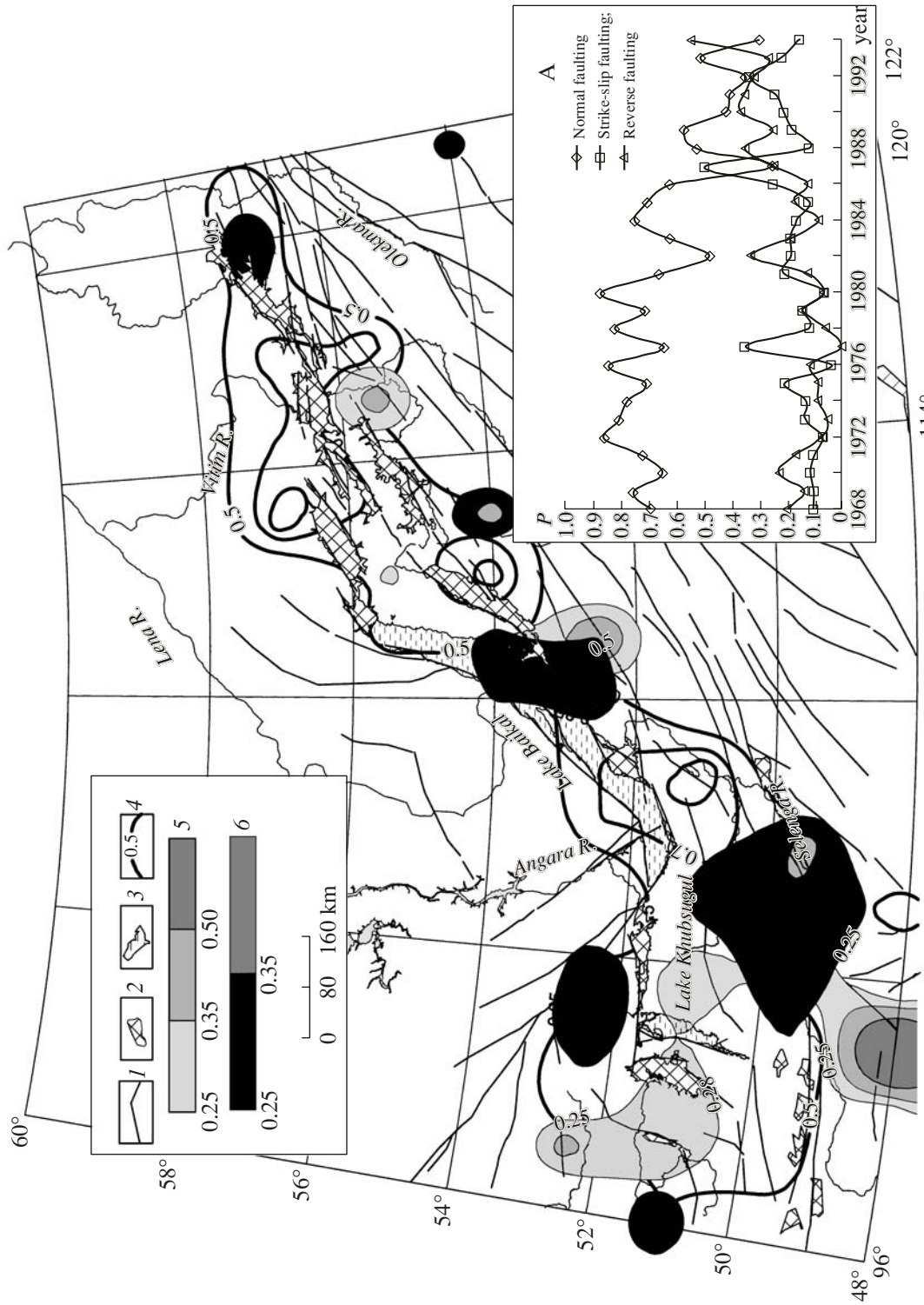

Fig. 2. Chart of contour lines of the realization probability of normal faulting, strike-slip faulting, and reverse faulting. Inset (A) presents graphs of the annual mean realization probability (P) of normal faulting, strike-slip faulting, and reverse faulting. (*1*) Faults; (*2*) depressions; (*3*) lakes; (*4*) contour lines of the realization probability of normal faulting (P_N); (*5*, *6*) scales of the realization probability of strike-slip faulting and reverse faulting (P_S and P_R, respectively).

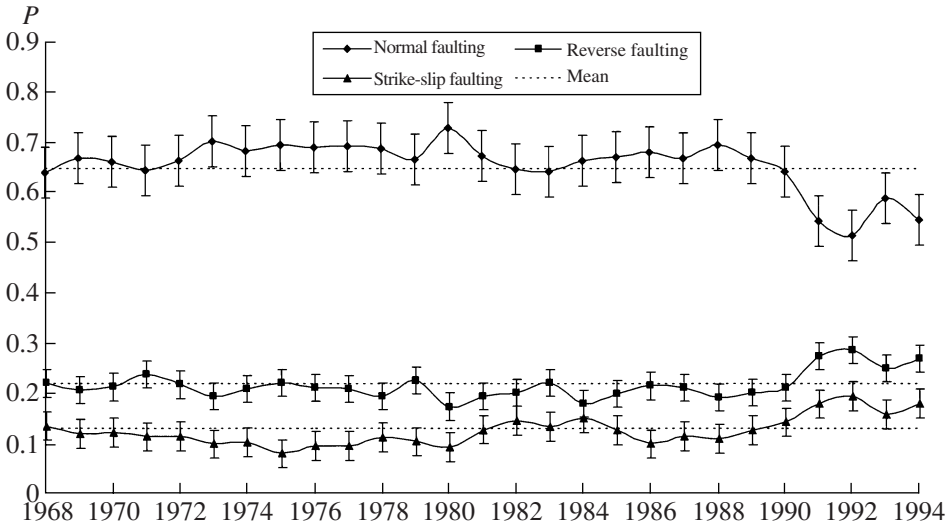

Fig. 3. Graphs of annual mean realization probability (P) based on the data on seismic moments of shocks in the Baikal region with $K_P \geq 8$.

bility of reverse faulting increased to $P_R \approx 0.55$, while $P_N \approx 0.30$ and $P_S \approx 0.15$.

Figure 3 shows the graphs of probability P based on the data of seismic moments of shocks with $K_P \geq 8$ recorded in the BRS from 1968 to 1994 to compare the dynamics of P_N, P_S, and P_R in the sources of weak and large earthquakes. One can see that, in general, the rifting regime dominates in the region at a mean level of $P_N \approx 0.65$ with an increase in 1980 and a decrease in the early 1990s at a level of two standard deviations. Strike-slip and reverse faultings make up approximately one-third of the shocks at a mean probability equal to $P_S \approx 0.22$ and $P_R \approx 0.13$, respectively. Comparison of Fig. 3 with the graph in Fig. 2 (inset A) shows a close correlation between the main tendencies in the behavior of P, but there are some differences in details. For example, it is seen in Fig. 3 that the time trend of the graphs of P is insignificant. However, the investigation of the probability dynamics separately for the shocks of each energy class demonstrated that the slope of the trends increases sequentially. In the first half of the 1990s, shocks with $K_P \geq 10$ show an intersection of probability trends P_N, P_S, and P_R similarly to the graphs in Fig. 2 (inset A). Such sequential variation in the slope of trends with an increase in the energy class can point to the time shift in the formation of different types of motions in the sources of large earthquakes. It is noteworthy that the trend of the graph of P_N changes most dynamically. Usually, the slope of the trend of P_R is steeper than the slope of P_S.

Figure 4 presents the graphs of probability P based on the data of seismic moments of shocks with $K_P = 8$, $K_P = 9$, …, and $K_P = 14$ recorded in the BRS from 1968 to 1994 to demonstrate the dependence of probabilities P_N, P_S, and P_R on the energy class of earthquakes. The graphs show the static probability calculated from the complete sampling of data for each K_P in 1968–1994. They also show dynamic probability, which is defined as the mean value over time of the annual probability of shocks of each class during the interval 1968–1994. It is clear that the equality between the static and dynamic probabilities should point to the ergodicity and stationarity of P in time. The complex form of graphs in Fig. 4 attracts attention. The static probability of shocks with $K_P = 10$, 13, and 14 decreases to a level of $P_N \approx 0.5$, while the mean level for other classes is $P_N \approx 0.65$. Variations in P_S and P_R are less significant in the range of weak shocks $P_S > P_R$, $P_S \approx P_R$ at $K_P = 10$–11, and $P_S < P_R$ at $K_P \geq 12$. The static and dynamic probabilities almost coincide for the shocks with $K_P \leq 11$, which evi-

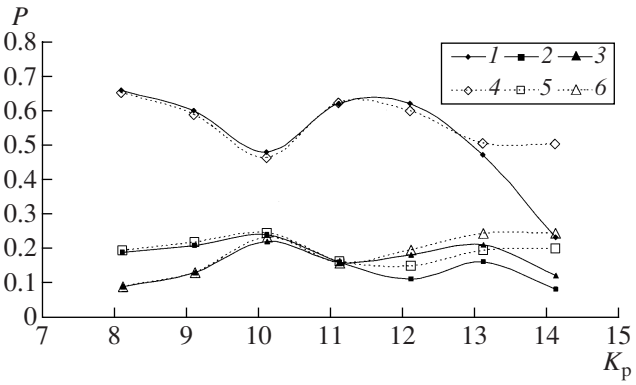

Fig. 4. Dependence of the realization probability of normal faulting P_N, strike-slip faulting P_S, and reverse faulting P_R on energy class K_P of earthquakes in the Baikal region. (*1–3*) Dynamic probability; (4–6) static probability.

dences that rifting stably dominates in this range of energy class of shocks. The dynamic probability decreases for larger earthquakes, possibly reflecting the fact of greater instability of stresses in the lithosphere of the BRS at the hierarchic level of large seismic events. It is seen that dynamic probabilities of shocks with different types of motions become closer at $K_P = 14$. This phenomenon reflects the sense of P presentation not only as the static probability, but also as the real probability of the estimate characterizing the random character of the seismic process of large earthquakes. The observed tendency of convergence of graphs of P_N, P_S, and P_R with increasing energy class indicates that the realization probability of different types of motions in the sources of large earthquakes in the BRS with $K_P > 14$ can be comparable.

Modern concepts about earthquakes as a phenomenon of instantaneous destruction of rocks as a fracture in response to gradient tectonic stresses form the ideas about local instability of the stressed-strained state of the medium, as well as the stochastic and fractal character of the distribution of stresses and strains in the lithosphere [13]. Hence, reconstruction of the stressed-strained state of the lithosphere of active regions and fractures by the methods of source seismology should use the results of processing of the parameters of earthquake sources in the full range of the lengths of rupture-defects in the lithosphere. The current research on the parameters of sources of large earthquakes is a necessary addition to the complex of works devoted to the investigation and reconstruction of the modern stressed state of the lithosphere in the BRS. The results of reconstruction of the stressed state of the medium in the lithosphere of the BRS based on the data about seismic moments of large earthquakes agree well with the results of spatiotemporal reconstruction of the stressed state based on the focal mechanisms of large earthquakes and seismic moments of moderate and weak shocks.

ACKNOWLEDGMENTS

This work was supported by the Russian Foundation for Basic Research, (project no. 05-05-97206p_Baikal, 06-05-64120-a).

REFERENCES

1. *Modern Dynamics of the Lithosphere of Continents* (Nedra, Moscow, 1995) [in Russian].
2. N. V. Solonenko and V. I. Mel'nikova, Geol. Geofiz. **35** (11), 99 (1994).
3. V. I. Mel'nikova and N. A. Radziminovich, Geol. Geofiz. **39**, 1598 (1998).
4. S. I. Golenetskii, Geol. Geofiz. **39**, 260 (1998).
5. A. V. Klyuchevskii, Dokl. Earth Sci. **385**, 551 (2002) [Dokl. Akad. Nauk **384**, 687 (2002)].
6. A. V. Klyuchevskii, Dokl. Earth Sci. **389**, 403 (2003) [Dokl. Akad. Nauk **389**, 398 (2003)].
7. A. V. Klyuchevskii and V. M. Dem'yanovich, Izv. Phys. Solid Earth **42**, 416, (2006) [Izv. Ross. Akad. Nauk, Fiz. Zemli, No. 5, 65 (2006)].
8. J. N. Brune, J. Geophys. Res. **75**, 4997 (1970).
9. A. V. Klyuchevskii, J. Geodyn. **37** (2), 155 (2004).
10. F. F. Aptikaev, Yu. F. Kopnichev, and A. V. Klyuchevskii, Dokl. Akad. Nauk SSSR **247**, 822 (1979).
11. Yu. F. Kopnichev and G. L. Shpil'ker, Izv. Akad. Nauk SSSR, Fiz. Zemli, No. 9, 3 (1980).
12. M. L. Zoback, J. Geophys. Res. **97** (B8), 11703 (1992).
13. *International Handbook of Earthquake and Engineering Seismology*, Ed. by W.H.K. Lee, H. Kanamori, P.C. Jennings, and C. Kisslinger, Part A (Academic, Amsterdam, 2002).